Chin. Ann. Math.
34B(2), 2013, 237–254
DOI: 10.1007/s11401-013-0764-1

Chinese Annals of Mathematics, Series B

On the Numerical Solution to a Nonlinear Wave Equation Associated with the First Painlevé Equation: an Operator-Splitting Approach

Roland GLOWINSKI[1] Annalisa QUAINI[2]

(*In honor of the scientific heritage of Jacques-Louis Lions*)

Abstract The main goal of this article is to discuss the numerical solution to a nonlinear wave equation associated with the first of the celebrated Painlevé transcendent ordinary differential equations. In order to solve numerically the above equation, whose solutions blow up in finite time, the authors advocate a numerical methodology based on the Strang's symmetrized operator-splitting scheme. With this approach, one can decouple nonlinearity and differential operators, leading to the alternate solution at every time step of the equation as follows: (i) The first Painlevé ordinary differential equation, (ii) a linear wave equation with a constant coefficient. Assuming that the space dimension is two, the authors consider a fully discrete variant of the above scheme, where the space-time discretization of the linear wave equation sub-steps is achieved via a Galerkin/finite element space approximation combined with a second order accurate centered time discretization scheme. To handle the nonlinear sub-steps, a second order accurate centered explicit time discretization scheme with adaptively variable time step is used, in order to follow accurately the fast dynamic of the solution before it blows up. The results of numerical experiments are presented for different coefficients and boundary conditions. They show that the above methodology is robust and describes fairly accurately the evolution of a rather "violent" phenomenon.

Keywords Painlevé equation, Nonlinear wave equation, Blow-up solution, Operator-Splitting
2000 MR Subject Classification 35L70, 65N06

1 Introduction

Although discovered from purely mathematical considerations, the six Painlevé "transcendent" ordinary differential equations arise in a variety of important physical applications (from plasma physics to quantum gravity), motivating the Painlevé project presented in [1], whose goal is to explore the various aspects of the six Painlevé equations. There is an abundant literature concerning the Painlevé equations (see [2–4] and the references therein). Surprisingly, very few of the related publications are of numerical nature, with notable exceptions being [4–5],

Manuscript received August 14, 2012.
[1]Department of Mathematics, University of Houston, 4800 Calhoun Rd, Houston (TX) 77204, USA. Laboratoire Jacques-Louis Lions, Universit Pierre et Marie Curie, 4, Place Jussieu, 75252 Paris CEDEX 05, France. E-mail: roland@math.uh.edu
[2]Department of Mathematics, University of Houston, 4800 Calhoun Rd, Houston (TX) 77204, USA. E-mail: quaini@math.uh.edu

which also contain additional references on the numerical solution to the Painlevé equations. Our goal in this article is, in some sense, more modest, since it is to associate with the first Painlevé equation

$$\frac{\mathrm{d}^2 y}{\mathrm{d}t^2} = 6y^2 + t, \tag{1.1}$$

and the following nonlinear wave equation:

$$\frac{\partial^2 u}{\partial t^2} - c^2 \nabla^2 u = 6u^2 + t \quad \text{in } \Omega \times (0, T_{\max}), \tag{1.2}$$

and to discuss the numerical solution to (1.2). Actually, we are going to consider the numerical solution to two initial/boundary value problems associated with (1.2), namely, we supplement (1.2) with initial conditions and pure homogeneous Dirichlet boundary conditions (resp. mixed Dirichlet-Sommerfeld boundary conditions), that is

$$\begin{cases} u = 0 & \text{on } \partial\Omega \times (0, T_{\max}), \\ u(0) = u_0, & \dfrac{\partial u}{\partial t}(0) = u_1, \end{cases} \tag{1.3}$$

(resp.

$$\begin{cases} u = 0 & \text{on } \Gamma_0 \times (0, T_{\max}), \\ \dfrac{1}{c}\dfrac{\partial u}{\partial t} + \dfrac{\partial u}{\partial n} = 0 & \text{on } \Gamma_1 \times (0, T_{\max}), \\ u(0) = u_0, & \dfrac{\partial u}{\partial t}(0) = u_1). \end{cases} \tag{1.4}$$

In (1.2)–(1.4), we have

(i) $c\,(> 0)$ is the speed of the propagation of the linear wave solutions to the equation

$$\frac{\partial^2 u}{\partial t^2} - c^2 \nabla^2 u = 0.$$

(ii) Ω is a bounded domain of $\mathbb{R}^d$, and $\partial\Omega$ is its boundary.

(iii) Γ_0 and Γ_1 are two disjoint non-empty subsets of $\partial\Omega$ satisfying $\Gamma_0 \cup \Gamma_1 = \partial\Omega$.

(iv) $\phi(t)$ denotes the function $x \to \phi(x, t)$.

The two problems under consideration are of multi-physics (reaction-propagation type) and multi-time scales nature. Thus, it makes sense to apply an operator-splitting method for the solutions to (1.2), (1.3) and (1.2), (1.4), in order to decouple the nonlinearity and differential operators and to treat the resulting sub-initial value problems with appropriate (and necessarily variable) time discretization sub-steps. Among the available operator-splitting methods, we chose the Strang's symmetrized operator-splitting scheme (introduced in [6]), because it provides a good compromise between accuracy and robustness as shown in [7–9] (and references therein).

The article is structured as follows. In Section 2, we discuss the time discretization of the problems (1.2), (1.3) and (1.2), (1.4) by the Strang's symmetrized scheme. In Sections 3 and 4, we discuss the solution to the initial value subproblems originating from the splitting, and the discussion includes the finite element approximation of the linear wave steps and the adaptive in time solution to the nonlinear ODE steps. In Section 5, we present the results of numerical experiments validating the numerical methodology discussed in the previous sections. In this section, we also investigate the influence of c and of the boundary conditions on the behavior of the solutions.

Remark 1.1 Strictly speaking, it is the solutions to the Painlevé equations which are transcendent, not the equations themselves.

Remark 1.2 This article is dedicated to J. L. Lions. We would like to mention that one can find, in Chapter 1 of his book celebrated in 1969 (see [10]), a discussion and further references on the existence and the non-existence of solutions to the following nonlinear wave problem:

$$\begin{cases} \dfrac{\partial^2 u}{\partial t^2} - \nabla^2 u = u^2 & \text{in } \Omega \times (0, T_{\max}), \\ u = 0 & \text{on } \partial\Omega \times (0, T_{\max}), \\ u(0) = u_0, \quad \dfrac{\partial u}{\partial t}(0) = u_1, \end{cases} \tag{1.5}$$

which is a related and simpler variant of problem (1.2), (1.3). The numerical methods discussed in this article can easily handle problem (1.5).

Remark 1.3 The numerical methodology discussed here can be applied more or less easily to other nonlinear wave equations of the following type:

$$\frac{\partial^2 u}{\partial t^2} - c^2 \nabla^2 u = f\Big(u, \frac{\partial u}{\partial t}, x, t\Big).$$

2 Application of the Strang's Symmetrized Operator-Splitting Scheme to the Solution to Problems (1.2), (1.3) and (1.2), (1.4)

2.1 A brief discussion of the Strang's operator-splitting scheme

Although the Strang's symmetrized scheme is quite well-known, it may be useful to present briefly this scheme before applying it to the solution to problems (1.2), (1.3) and (1.2), (1.4). Our presentation follows closely the ones in [7, Chapter 6] and [11].

Let us consider thus the following non-autonomous abstract initial value problem (taking place in a Banach space, for example):

$$\begin{cases} \dfrac{\mathrm{d}\phi}{\mathrm{d}t} + A(\phi, t) + B(\phi, t) = 0 \quad \text{in } (0, T_{\max}), \\ \phi(0) = \phi_0, \end{cases} \tag{2.1}$$

where the operators A and B can be nonlinear and even multivalued (in which case one has to replace $= 0$ by $\ni 0$ in (2.1)). Let Δt be a time-step (fixed, for simplicity), and let us denote $(n+\alpha)\Delta t$ by $t^{n+\alpha}$. When applied to the time discretization of (2.1), the basic Strang's symmetrized scheme reads as follows:

Step 1 Set

$$\phi^0 = \phi_0. \tag{2.2}$$

For $n \geq 0$, ϕ^n being known, compute ϕ^{n+1} as below.

Step 2 Set $\phi^{n+\frac{1}{2}} = \phi(t^{n+\frac{1}{2}})$, where ϕ is the solution to

$$\begin{cases} \dfrac{\mathrm{d}\phi}{\mathrm{d}t} + A(\phi, t) = 0 \quad \text{in } (t^n, t^{n+\frac{1}{2}}), \\ \phi(t^n) = \phi^n. \end{cases} \tag{2.3}$$

Step 3 Set $\widehat{\phi}^{n+\frac{1}{2}} = \phi(\Delta t)$, where ϕ is the solution to

$$\begin{cases} \dfrac{\mathrm{d}\phi}{\mathrm{d}t} + B(\phi, t^{n+\frac{1}{2}}) = 0 \quad \text{in } (0, \Delta t), \\ \phi(0) = \phi^{n+\frac{1}{2}}. \end{cases} \tag{2.4}$$

Step 4 Set $\phi^{n+1} = \phi(t^{n+1})$, where ϕ is the solution to

$$\begin{cases} \dfrac{\mathrm{d}\phi}{\mathrm{d}t} + A(\phi, t) = 0 \quad \text{in } (t^{n+\frac{1}{2}}, t^{n+1}), \\ \phi(t^{n+\frac{1}{2}}) = \widehat{\phi}^{n+\frac{1}{2}}. \end{cases} \tag{2.5}$$

If the operators A and B are smooth functions of their arguments, the above scheme is second order accurate. In addition to [6–9, 11], useful information about the operator-splitting solution to partial differential equations can be found in [12–16] (and references therein).

2.2 Application to the solution to the nonlinear wave problem (1.2), (1.3)

In order to apply the symmetrized scheme to the solution to (1.2), (1.3), we reformulate the above problem as a first order in time system by introducing the function $p = \dfrac{\partial u}{\partial t}$. We obtain that

$$\begin{cases} \dfrac{\partial u}{\partial t} - p = 0 & \text{in } \Omega \times (0, T_{\max}), \\ \dfrac{\partial p}{\partial t} - c^2 \nabla^2 u = 6u^2 + t & \text{in } \Omega \times (0, T_{\max}) \end{cases} \tag{2.6}$$

with boundary and initial conditions

$$\begin{cases} u = 0 \quad \text{on } \partial\Omega \times (0, T_{\max}), \\ u(0) = u_0, \quad p(0) = u_1. \end{cases} \tag{2.7}$$

Clearly, (2.6), (2.7) is equivalent to (1.2), (1.3).

With Δt as in Subsection 2.1, we introduce $\alpha, \beta \in (0,1)$ such that $\alpha + \beta = 1$. Applying scheme (2.2)–(2.5) to the solution of (2.6), (2.7), we obtain the following:

Step 1 Set

$$u^0 = u_0, \quad p^0 = u_1. \tag{2.8}$$

For $n \geq 0$, $\{u^n, p^n\}$ being known, compute $\{u^{n+1}, p^{n+1}\}$ as below.

Step 2 Set $u^{n+\frac{1}{2}} = u(t^{n+\frac{1}{2}})$, $p^{n+\frac{1}{2}} = p(t^{n+\frac{1}{2}})$, where $\{u, p\}$ is the solution to

$$\begin{cases} \dfrac{\partial u}{\partial t} - \alpha p = 0 \quad \text{in } \Omega \times (t^n, t^{n+\frac{1}{2}}), \\ \dfrac{\partial p}{\partial t} = 6u^2 + t \quad \text{in } \Omega \times (t^n, t^{n+\frac{1}{2}}), \\ u(t^n) = u^n, \quad p(t^n) = p^n. \end{cases} \tag{2.9}$$

Step 3 Set $\widehat{u}^{n+\frac{1}{2}} = u(\Delta t)$, $\widehat{p}^{n+\frac{1}{2}} = p(\Delta t)$, where $\{u, p\}$ is the solution to

$$\begin{cases} \dfrac{\partial u}{\partial t} - \beta p = 0 & \text{in } \Omega \times (0, \Delta t), \\ \dfrac{\partial p}{\partial t} - c^2 \nabla^2 u = 0 & \text{in } \Omega \times (0, \Delta t), \\ u = 0 & \text{on } \partial\Omega \times (0, \Delta t), \\ u(0) = u^{n+\frac{1}{2}}, \quad p(0) = p^{n+\frac{1}{2}}. \end{cases} \tag{2.10}$$

Step 4 Set $u^{n+1} = u(t^{n+1})$, $p^{n+1} = p(t^{n+1})$, where $\{u, p\}$ is the solution to

$$\begin{cases} \dfrac{\partial u}{\partial t} - \alpha p = 0 \quad \text{in } \Omega \times (t^{n+\frac{1}{2}}, t^{n+1}), \\ \dfrac{\partial p}{\partial t} = 6u^2 + t \quad \text{in } \Omega \times (t^{n+\frac{1}{2}}, t^{n+1}), \\ u(t^{n+\frac{1}{2}}) = \widehat{u}^{n+\frac{1}{2}}, \quad p(t^{n+\frac{1}{2}}) = \widehat{p}^{n+\frac{1}{2}}. \end{cases} \tag{2.11}$$

By the partial elimination of p, (2.8)–(2.11) reduces to the following:
Step 1 As in (2.8).
For $n \geq 0$, $\{u^n, p^n\}$ being known, compute $\{u^{n+1}, p^{n+1}\}$ as below.
Step 2 Set $u^{n+\frac{1}{2}} = u(t^{n+\frac{1}{2}})$, $p^{n+\frac{1}{2}} = \frac{1}{\alpha}\frac{\partial u}{\partial t}(t^{n+\frac{1}{2}})$, where u is the solution to

$$\begin{cases} \dfrac{\partial^2 u}{\partial t^2} = \alpha(6u^2 + t) \quad \text{in } \Omega \times (t^n, t^{n+\frac{1}{2}}), \\ u(t^n) = u^n, \quad \dfrac{\partial u}{\partial t}(t^n) = \alpha p^n. \end{cases} \tag{2.12}$$

Step 3 Set $\widehat{u}^{n+\frac{1}{2}} = u(\Delta t)$, $\widehat{p}^{n+\frac{1}{2}} = \frac{1}{\beta}\frac{\partial u}{\partial t}(\Delta t)$, where u is the solution to

$$\begin{cases} \dfrac{\partial^2 u}{\partial t^2} - \beta c^2 \nabla^2 u = 0 \quad \text{in } \Omega \times (0, \Delta t), \\ u = 0 \qquad\qquad\qquad \text{on } \partial\Omega \times (0, \Delta t), \\ u(0) = u^{n+\frac{1}{2}}, \quad \dfrac{\partial u}{\partial t}(0) = \beta p^{n+\frac{1}{2}}. \end{cases} \tag{2.13}$$

Step 4 Set $u^{n+1} = u(t^{n+1})$, $p^{n+1} = \frac{1}{\alpha}\frac{\partial u}{\partial t}(t^{n+1})$, where u is the solution to

$$\begin{cases} \dfrac{\partial^2 u}{\partial t^2} = \alpha(6u^2 + t) \quad \text{in } \Omega \times (t^{n+\frac{1}{2}}, t^{n+1}), \\ u(t^{n+\frac{1}{2}}) = \widehat{u}^{n+\frac{1}{2}}, \quad \dfrac{\partial u}{\partial t}(t^{n+\frac{1}{2}}) = \alpha \widehat{p}^{n+\frac{1}{2}}. \end{cases} \tag{2.14}$$

2.3 Application to the solution to the nonlinear wave problem (1.2), (1.4)

Proceeding as in Subsection 2.2, we introduce $p = \frac{\partial u}{\partial t}$ in order to reformulate (1.2), (1.4) as the first order in time system. We obtain the system (2.6) supplemented with the following boundary and initial conditions:

$$\begin{cases} u(0) = 0 \qquad\quad \text{on } \Gamma_0 \times (0, T_{\max}), \\ \dfrac{p}{c} + \dfrac{\partial u}{\partial n} = 0 \quad \text{on } \Gamma_1 \times (0, T_{\max}), \\ u(0) = u_0, \quad p(0) = u_1. \end{cases} \tag{2.15}$$

Applying scheme (2.2)–(2.5) to the solution to the equivalent problem (2.6), (2.15), we obtain the following:
Step 1 As in (2.8).
For $n \geq 0$, $\{u^n, p^n\}$ being known, compute $\{u^{n+1}, p^{n+1}\}$ as below.
Step 2 As in (2.12).

Step 3 Set $\widehat{u}^{n+\frac{1}{2}} = u(\Delta t)$, $\widehat{p}^{n+\frac{1}{2}} = \frac{1}{\beta}\frac{\partial u}{\partial t}(\Delta t)$, where u is the solution to

$$\begin{cases} \dfrac{\partial^2 u}{\partial t^2} - \beta c^2 \nabla^2 u = 0 & \text{in } \Omega \times (0, \Delta t), \\ u = 0 & \text{on } \Gamma_0 \times (0, \Delta t), \\ \dfrac{1}{\beta c}\dfrac{\partial u}{\partial t} + \dfrac{\partial u}{\partial n} = 0 & \text{on } \Gamma_1 \times (0, \Delta t), \\ u(0) = u^{n+\frac{1}{2}}, \quad \dfrac{\partial u}{\partial t}(0) = \beta p^{n+\frac{1}{2}}. \end{cases} \tag{2.16}$$

Step 4 As in (2.14).

3 On the Numerical Solution to the Sub-initial Value Problems (2.13) and (2.16)

3.1 Some generalities

Since problem (2.13) is the particular case of (2.16) corresponding to $\Gamma_1 = \emptyset$, we are going to consider the second problem only. This linear wave problem is a particular case of

$$\begin{cases} \dfrac{\partial^2 \phi}{\partial t^2} - \beta c^2 \nabla^2 \phi = 0 & \text{in } \Omega \times (t_0, t_f), \\ \phi = 0 & \text{on } \Gamma_0 \times (t_0, t_f), \\ \dfrac{1}{\beta c}\dfrac{\partial \phi}{\partial t} + \dfrac{\partial \phi}{\partial n} = 0 & \text{on } \Gamma_1 \times (t_0, t_f), \\ \phi(t_0) = \phi_0, \quad \dfrac{\partial \phi}{\partial t}(t_0) = \phi_1. \end{cases} \tag{3.1}$$

Assuming that ϕ_0 and ϕ_1 have enough regularity, a variational (weak) formulation of problem (3.1) is given by the following: Find $\phi(t) \in V_0$, a.e. on (t_0, t_f), such that

$$\begin{cases} \Big\langle \dfrac{\partial^2 \phi}{\partial t^2}, \theta \Big\rangle + \beta c^2 \displaystyle\int_\Omega \nabla\phi \cdot \nabla\theta \mathrm{d}x + c \int_{\Gamma_1} \dfrac{\partial \phi}{\partial t}\theta \mathrm{d}\Gamma = 0, \quad \forall \theta \in V_0, \\ \phi(t_0) = \phi_0, \quad \dfrac{\partial \phi}{\partial t}(t_0) = \phi_1, \end{cases} \tag{3.2}$$

where

(i) V_0 is the Sobolev space defined by

$$V_0 = \{\theta \mid \theta \in H^1(\Omega),\ \theta = 0 \text{ on } \Gamma_0\}, \tag{3.3}$$

(ii) $\langle \cdot, \cdot \rangle$ is the duality pairing between V_0' (the dual of V_0) and V_0, coinciding with the canonical inner product of $L^2(\Omega)$ if the first argument is smooth enough,

(iii) $\mathrm{d}x = \mathrm{d}x_1 \cdots \mathrm{d}x_d$.

3.2 A finite element method for the space discretization of the linear wave problem (3.1)

From now on, we are going to assume that Ω is a bounded polygonal domain of $\mathbb{R}^2$. Let $\mathcal{T}_h$ be a classical finite element triangulation of Ω, as considered in [17, Appendix 1] and related references therein. We approximate the space V_0 in (3.3) by

$$V_{0h} = \{\theta \mid \theta \in C^0(\overline{\Omega}),\ \theta|_{\Gamma_0} = 0,\ \theta|_K \in \mathbb{P}_1,\ \forall K \in \mathcal{T}_h\}, \tag{3.4}$$

where $\mathbb{P}_1$ is the space of the polynomials of two variables of degree ≤ 1. If $\Gamma_1 \neq \emptyset$, the points at the interface of Γ_0 and Γ_1 have to be (for consistency reasons) vertices of $\mathcal{T}_h$, at which any element of V_{0h} has to vanish. It is natural to approximate the wave problem (3.2) as follows: Find $\phi_h(t) \in V_{0h}$, a.e. on $(t_0, t_f]$, such that

$$\begin{cases} \displaystyle\int_\Omega \frac{\partial^2 \phi_h}{\partial t^2}\theta \mathrm{d}x + \beta c^2 \int_\Omega \nabla\phi_h \cdot \nabla\theta \mathrm{d}x + c\int_{\Gamma_1} \frac{\partial \phi_h}{\partial t}\theta \mathrm{d}\Gamma = 0, \quad \forall \theta \in V_{0h}, \\ \phi_h(t_0) = \phi_{0h}, \quad \dfrac{\partial \phi_h}{\partial t}(t_0) = \phi_{1h}, \end{cases} \tag{3.5}$$

where ϕ_{0h} and ϕ_{1h} belong to V_{0h}, and approximate ϕ_0 and ϕ_1, respectively.

In order to formulate (3.5) as a second order in time system of linear ordinary differential equations, we introduce first the set $\Sigma_{0h} = \{P_j\}_{j=1}^{N_{0h}}$ of the vertices of $\mathcal{T}_h$, which do not belong to $\overline{\Gamma}_0$, and associate with it the following basis of V_{0h}:

$$\mathcal{B}_{0h} = \{w_j\}_{j=1}^{N_{0h}},$$

where the basis function w_j is defined by

$$w_j \in V_{0h}, \quad w_j(P_j) = 1, \quad w_j(P_k) = 0, \quad \forall k \in \{1, \cdots, N_{0h}\},\ k \neq j.$$

Expanding the solution ϕ_h to (3.5) over the above basis, we obtain

$$\phi_h(t) = \sum_{j=1}^{N_{0h}} \phi_h(P_j, t) w_j.$$

Denoting $\phi_h(P_j, t)$ by $\phi_j(t)$ and the N_{0h}-dimensional vector $\{\phi_j(t)\}_{j=1}^{N_{0h}}$ by $\mathbf{\Phi}_h(t)$, we can easily show that the approximated problem (3.5) is equivalent to the following ordinary differential system:

$$\begin{cases} \mathbf{M}_h \ddot{\mathbf{\Phi}}_h + \beta c^2 \mathbf{A}_h \mathbf{\Phi}_h + c\mathbf{C}_h \dot{\mathbf{\Phi}}_h = \mathbf{0} \quad \text{on } (t_0, t_f), \\ \mathbf{\Phi}_h(t_0) = \mathbf{\Phi}_{0h}\ (= (\phi_{0h}(P_j))_{j=1}^{N_{0h}}), \quad \dot{\mathbf{\Phi}}_h(t_0) = \mathbf{\Phi}_{1h}\ (= (\phi_{1h}(P_j))_{j=1}^{N_{0h}}), \end{cases} \tag{3.6}$$

where the mass matrix $\mathbf{M}_h$, the stiffness matrix $\mathbf{A}_h$, and the damping matrix $\mathbf{C}_h$ are defined by

$$\begin{aligned} \mathbf{M}_h &= (m_{ij})_{1\leq i,j\leq N_{0h}} \quad \text{with } m_{ij} = \int_\Omega w_i w_j \mathrm{d}x, \\ \mathbf{A}_h &= (a_{ij})_{1\leq i,j\leq N_{0h}} \quad \text{with } a_{ij} = \int_\Omega \nabla w_i \cdot \nabla w_j \mathrm{d}x, \\ \mathbf{C}_h &= (c_{ij})_{1\leq i,j\leq N_{0h}} \quad \text{with } c_{ij} = \int_{\Gamma_1} w_i w_j \mathrm{d}\Gamma, \end{aligned}$$

respectively.

The matrices $\mathbf{M}_h$ and $\mathbf{A}_h$ are sparse and positive definite, while matrix $\mathbf{C}_h$ is "very" sparse and positive semi-definite. Indeed, if P_i and P_j are not neighbors, i.e., they are not vertices of a same triangle of $\mathcal{T}_h$, we have $m_{ij} = 0$, $a_{ij} = 0$ and $c_{ij} = 0$. All these matrix entries can be computed exactly, using, for example, the two-dimensional Simpson's rule for the m_{ij} and the one-dimensional Simpson's rule for the c_{ij}. Since ∇w_i and ∇w_j are piecewise constant, computing a_{ij} is (relatively) easy (see [7, Chapter 5] for more details on these calculations).

Remark 3.1 Using the trapezoidal rule, instead of Simpson's one, to compute the m_{ij} and c_{ij} brings simplification as follows: The resulting $\mathbf{M}_h$ and $\mathbf{C}_h$ will be diagonal matrices, retaining the positivity properties of their Simpson's counterparts. The drawback is some accuracy loss associated with this simplification.

3.3 A centered second order finite difference scheme for the time discretization of the initial value problem (3.6)

Let Q be a positive integer (≥ 3, in practice). We associate with Q a time discretization step $\tau = \frac{t_f - t_0}{Q}$. After dropping the subscript h, a classical time discretization scheme for problem (3.6) reads as: Set

$$\mathbf{\Phi}^0 = \mathbf{\Phi}_0, \quad \mathbf{\Phi}^1 - \mathbf{\Phi}^{-1} = 2\tau\mathbf{\Phi}_1, \tag{3.7}$$

then for $q = 0, \cdots, Q$, compute $\mathbf{\Phi}^{q+1}$ by

$$\mathbf{M}(\mathbf{\Phi}^{q+1} + \mathbf{\Phi}^{q-1} - 2\mathbf{\Phi}^q) + \beta c^2\tau^2\mathbf{A}\mathbf{\Phi}^q + c\frac{\tau}{2}\mathbf{C}(\mathbf{\Phi}^{q+1} - \mathbf{\Phi}^{q-1}) = \mathbf{0}. \tag{3.8}$$

It follows from [7, Chapter 6] that the above second order accurate scheme is stable if the following condition holds:

$$\tau < \frac{2}{c\sqrt{\beta\lambda_{\max}}}, \tag{3.9}$$

where $\lambda_{\max}$ is the largest eigenvalue of $\mathbf{M}^{-1}\mathbf{A}$.

Remark 3.2 To obtain $\mathbf{\Phi}^{q+1}$ from (3.8), one has to solve a linear system associated with the symmetric positive definite matrix

$$\mathbf{M} + \frac{\tau}{2}c\mathbf{C}. \tag{3.10}$$

If the above matrix is diagonal from the use of the trapezoidal rule (see Remark 3.1), computing $\mathbf{\Phi}^{q+1}$ is particularly easy and the time discretization scheme (3.8) is fully explicit. Otherwise, scheme (3.8) is not explicit, strictly speaking. However, since matrix (3.10) is well conditioned, a conjugate gradient algorithm with diagonal preconditioning will have a very fast convergence, particularly if one uses $\mathbf{\Phi}^q$ to initialize the computation of $\mathbf{\Phi}^{q+1}$.

Remark 3.3 In order to initialize the discrete analogue of the initial value problem (2.14), we will use

$$\mathbf{\Phi}^Q \quad \text{and} \quad \frac{\alpha}{\beta}\frac{\mathbf{\Phi}^{Q+1} - \mathbf{\Phi}^{Q-1}}{2\tau}. \tag{3.11}$$

Remark 3.4 As the solution to the nonlinear wave problem under consideration gets closer to blow-up, the norms of the corresponding initial data in (3.7) will go to infinity. In order to off-set (partly, at least) the effect of round-off errors, we suggest the following normalization strategy:

(1) Denote by $\|\phi_{0h}\|_{0h}$ and $\|\phi_{1h}\|_{0h}$ the respective approximations of

$$\left(\int_\Omega |\phi_{0h}|^2 \mathrm{d}x\right)^{\frac{1}{2}} \quad \text{and} \quad \left(\int_\Omega |\phi_{1h}|^2 \mathrm{d}x\right)^{\frac{1}{2}}$$

obtained by the trapezoidal rule.

(2) Divide by $\max[1, \sqrt{\|\phi_{0h}\|_{0h}^2 + \|\phi_{1h}\|_{0h}^2}]$ the initial data $\mathbf{\Phi}_0$ and $\mathbf{\Phi}_1$ in (3.7).

(3) Apply the scheme (3.8) with normalized initial data to compute $\mathbf{\Phi}^{Q-1}$, $\mathbf{\Phi}^Q$ and $\mathbf{\Phi}^{Q+1}$.

(4) Prepare the initial data for the following nonlinear sub-step by multiplying (3.11) by the normalization factor $\max[1, \sqrt{\|\phi_{0h}\|_{0h}^2 + \|\phi_{1h}\|_{0h}^2}]$.

4 On the Numerical Solution to the Sub-initial Value Problems (2.12) and (2.14)

4.1 Generalities

From $n = 0$ until blow-up, we have to solve the initial value sub-problems (2.12) and (2.14) for almost every point of Ω. Following what we discussed in Section 3 (whose notation we keep), for the solution to the linear wave equation subproblems, we will consider only those nonlinear initial value sub-problems associated with the N_{0h} vertices of $\mathcal{T}_h$ not located on $\overline{\Gamma}_0$. Each of these sub-problem is of the following type:

$$\begin{cases} \dfrac{\mathrm{d}^2\phi}{\mathrm{d}t^2} = \alpha(6\phi^2 + t) \quad \text{in } (t_0, t_f), \\ \phi(t_0) = \phi_0, \quad \dfrac{\mathrm{d}\phi}{\mathrm{d}t}(t_0) = \phi_1 \end{cases} \tag{4.1}$$

with the initial data for (4.1) as in algorithms (2.8), (2.12), (2.16) and (2.14), after space discretization. A time discretization scheme of (4.1) with automatic adjustment of the time step will be discussed in the following section.

4.2 A centered scheme for the time discretization of (4.1)

Let M be a positive integer (> 2 in practice). With M, we associate a time discretization step $\sigma = \frac{t_f - t_0}{M}$. For the time discretization of the initial value problem (4.1), we suggest the following nonlinear variant of (3.8): Set

$$\phi^0 = \phi_0, \quad \phi^1 - \phi^{-1} = 2\sigma\phi_1,$$

then for $m = 0, \cdots, M$, compute ϕ^{m+1} by

$$\phi^{m+1} + \phi^{m-1} - 2\phi^m = \alpha\sigma^2(6|\phi^m|^2 + t^m) \tag{4.2}$$

with $t^m = t^0 + m\sigma$.

Considering the blowing-up properties of the solutions to the nonlinear wave problems (1.2), (1.3) and (1.2), (1.4), we expect that at one point in time, the solution to problem (4.1) will start growing very fast before becoming infinite. In order to track such a behavior, we have to decrease σ in (4.2), until the solution reaches some threshold at which we decide to stop computing (for the computational experiments reported in Section 5, we stop computing beyond 10^4). A practical method for the adaptation of the time step σ is described below.

4.3 On the dynamical adaptation of the time step σ

The starting point of our adaptive strategy will be the following observation: If ϕ is the solution to (4.1), at a time t before blow-up and for σ sufficiently small, we have (Taylor's expansion)

$$\begin{aligned} \phi(t+\sigma) &= \phi(t) + \sigma\dot{\phi}(t) + \frac{\sigma^2}{2}\ddot{\phi}(t) + \frac{\sigma^3}{6}\dddot{\phi}(t+\theta\sigma) \\ &= \phi(t) + \sigma\dot{\phi}(t) + \frac{\sigma^2}{2}\alpha(6|\phi(t)|^2 + t) + \sigma^3\alpha\Big(2\phi(t+\theta\sigma)\dot{\phi}(t+\theta\sigma) + \frac{1}{6}\Big) \end{aligned} \tag{4.3}$$

with $0 < \theta < 1$. Suppose that we drop the σ^3-term in the above expansion, and that we approximate by finite differences the resulted truncated expansion at $t = t^m$. Then we obtain

$$\phi^{m+1} = \phi^m + \sigma\frac{\phi^{m+1} - \phi^{m-1}}{2\sigma} + \frac{\sigma^2}{2}\alpha(6|\phi^m|^2 + t^m),$$

which is the explicit scheme (4.2). Moreover, from the expansion (4.3), we can derive the following estimate of the relative error at $t = t^{m+1}$:

$$E^{m+1} = \sigma^3 \alpha \frac{\left|(\phi^{m+1} + \phi^m)\frac{(\phi^{m+1}-\phi^m)}{\sigma}\right| + \frac{1}{6}}{\max[1, |\phi^{m+1}|]}.$$

Another possible estimator would be

$$\sigma^3 \alpha \frac{\left|(\phi^{m+1} + \phi^m)\frac{(\phi^{m+1}-\phi^m)}{\sigma}\right| + \frac{1}{6}}{\max\left[1, \frac{1}{2}|\phi^m + \phi^{m+1}|\right]}.$$

In order to adapt σ by using E^{m+1}, we may proceed as follows: If ϕ^{m+1} obtained from the scheme (4.2) verifies

$$E^{m+1} \leq \text{tol}, \tag{4.4}$$

keep integrating with σ as a time discretization step. If criterion (4.4) is not verified, we have two possible situations, one for $m = 0$ and one for $m \geq 1$. If $m = 0$:

- Divide σ by 2 as many times as necessary to have

$$E^1 \leq \frac{\text{tol}}{5}. \tag{4.5}$$

  Each time σ is divided by 2, double M accordingly.
- Still calling σ the first time step for which (4.5) holds after successive divisions by 2, apply scheme (4.2) to the solution to (4.1), with the new σ and the associated M.

If $m \geq 1$:

- Go to $t = t^{m-\frac{1}{2}} = t_0 + \left(m - \frac{1}{2}\right)\sigma$.
- $t^{m-\frac{1}{2}} \to t_0$, $\frac{\phi^{m-1}+\phi^m}{2} \to \phi_0$, $\frac{\phi^m - \phi^{m-1}}{\sigma} \to \phi_1$.
- $\sigma \to \frac{\sigma}{2}$.
- $2(M-m)+1 \to M$.
- Apply scheme (4.2) on the new interval (t_0, t_f). If criterion (4.4) is not verified, then proceed as in the case of $m = 0$.

For the numerical results reported in Section 5, we use tol $= 10^{-4}$.

Remark 4.1 In order to initialize the discrete analogues of the initial value problems (2.12), (2.13), we will use

$$\phi^M, \quad \frac{\phi^{M+1} - \phi^{M-1}}{2\sigma}$$

and

$$\phi^M, \quad \frac{\beta}{\alpha}\frac{\phi^{M+1} - \phi^{M-1}}{2\sigma},$$

respectively.

5 Numerical Experiments

5.1 Generalities

In this section, we are going to report on the results of numerical experiments concerning the solutions to the nonlinear wave problems (1.2), (1.3) and (1.2), (1.4). The role of these experiments is two-fold as follows: (i) Validate the numerical methodology discussed in Sections 2–4, (ii) investigate how c and the boundary conditions influence the solutions.

For both problems, we took $\Omega = (0,1)^2$. For the problem (1.2), (1.4), we took $\Gamma_1 = \{\{x_1, x_2\}, x_1 = 1, 0 < x_2 < 1\}$. The simplicity of the geometry suggests the use of finite differences for the space discretization. Actually, the finite difference schemes which we employ can be obtained via the finite element approximation discussed in Section 3, combined with the trapezoidal rule to compute the mass matrix $\mathbf{M}_h$ and the damping matrix $\mathbf{C}_h$. This requires that the triangulations which we employ are uniform like the one depicted in Figure 1.

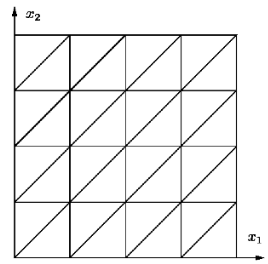

Figure 1 A uniform triangulation of Ω.

5.2 Numerical experiments for the nonlinear wave problem (1.2), (1.3)

Using well-known notation, we assume that the directional space discretization steps Δx_1 and Δx_2 are equal, and we denote by h their common value. We also assume that $h = \frac{1}{I+1}$, where I is a positive integer. For $0 \le i, j \le I+1$, we denote by M_{ij} the point $\{ih, jh\}$ and $u_{ij}(t) \simeq u(M_{ij}, t)$. Using finite differences, we obtain the following continuous in time, discrete in space analogue of the problem (1.2), (1.3):

$$\begin{cases} u_{ij}(0) = u_0(M_{ij}), \quad 0 \le i, j \le I+1, \\ \dot{u}_{ij}(0) = u_1(M_{ij}), \quad 1 \le i, j \le I, \\ \ddot{u}_{ij}(t) + \Big(\dfrac{c}{h}\Big)^2 (4u_{ij} - u_{i+1j} - u_{i-1j} - u_{ij+1} - u_{ij-1})(t) \\ \quad = 6|u_{ij}(t)|^2 + t \quad \text{on } (0, T_{\max}),\ 1 \le i, j \le I, \\ u_{kl}(t) = 0 \quad \text{on } (0, T_{\max}) \text{ if } M_{kl} \in \partial\Omega. \end{cases} \tag{5.1}$$

In (5.1), we assume that u_0 (resp. u_1) belongs to $C^0(\overline{\Omega}) \cap H_0^1(\Omega)$ (resp. $C^0(\overline{\Omega})$).

The application of the discrete analogue of the operator-splitting scheme (2.8), (2.12)–(2.14) to problem (5.1) leads to the solution at each time step of:

(i) a discrete linear wave problem of the following type:

$$\begin{cases} \phi_{ij}(t_0) = \phi_0(M_{ij}), \quad 0 \le i, j \le I+1, \\ \dot{\phi}_{ij}(t_0) = \phi_1(M_{ij}), \quad 1 \le i, j \le I, \\ \ddot{\phi}_{ij}(t) + \beta\Big(\dfrac{c}{h}\Big)^2 (4\phi_{ij} - \phi_{i+1j} - \phi_{i-1j} \\ \quad -\phi_{ij+1} - \phi_{ij-1})(t) = 0 \quad \text{on } (t_0, t_f),\ 1 \le i, j \le I, \\ \phi_{kl}(t) = 0 \quad \text{on } (t_0, t_f) \text{ if } M_{kl} \in \partial\Omega. \end{cases} \tag{5.2}$$

(ii) $2I^2$ nonlinear initial value problems (2 for each interior grid point M_{ij}) like (4.1).

The numerical solution of the problem (4.1) has been addressed in Subsections 4.2 and 4.3. Concerning problem (5.2), it follows from Section 3 that its time discrete analogue reads as follows: Set

$$\phi_{ij}^0 = \phi_0(M_{ij}), \quad 0 \le i,j \le I+1 \quad \text{and} \quad \phi_{ij}^1 - \phi_{ij}^{-1} = 2\tau\phi_1(M_{ij}), \quad 1 \le i,j \le I,$$

then, for $q = 0, \cdots, Q$, $1 \le i,j \le I$, we have

$$\begin{cases} \phi_{ij}^{q+1} + \phi_{ij}^{q-1} - 2\phi_{ij}^q + \beta\Big(\dfrac{\tau}{h}c\Big)^2 (4\phi_{ij}^q - \phi_{i+1j}^q - \phi_{i-1j}^q - \phi_{ij+1}^q - \phi_{ij-1}^q) = 0, \\ \phi_{kl}^{q+1} = 0 \quad \text{if } M_{kl} \in \partial\Omega \end{cases} \tag{5.3}$$

with $\tau = \frac{t_f - t_0}{Q}$. In the particular case of scheme (5.3), the stability condition (3.9) takes the following form:

$$\tau < \frac{h}{c\sqrt{2\beta}}. \tag{5.4}$$

For the numerical results presented below, we took

(i) $u_0 = 0$ and $u_1 = 0$.

(ii) c ranging from 0 to 1.5.

(iii) $\alpha = \beta = \frac{1}{2}$.

(iv) $Q = 3$.

(v) For $h = \frac{1}{100}$: $\Delta t = 10^{-2}$ for $c \in [0, 0.6]$; $\Delta t = 8 \times 10^{-3}$ for $c = 0.7, 0.8$; $\Delta t = 5 \times 10^{-3}$ for $c = 0.9, 1, 1.25$; $\Delta t = 10^{-3}$ for $c = 1.5$.

(vi) For $h = \frac{1}{150}$: $\Delta t = 6 \times 10^{-3}$ for $c \in [0, 0.6]$; $\Delta t = 4 \times 10^{-3}$ for $c = 0.7, 0.8$; $\Delta t = 3 \times 10^{-3}$ for $c = 0.9, 1, 1.25$; $\Delta t = 6 \times 10^{-4}$ for $c = 1.5$.

We initialize with $M = 3$ (see Section 4.2), and then adapt M following the procedure described in Subsection 4.3.

We consider that the blow-up time is reached as soon as the maximum value of the discrete solution reaches 10^4. Let us remark that the numerical results obtained with $h = \frac{1}{100}$ and $h = \frac{1}{150}$ (and the respective associated values of Δt) are essentially identical.

In Figure 2, we report the results obtained by our methodology when $c = 0$. They compare quite well with the results reported by Wikipedia [18].

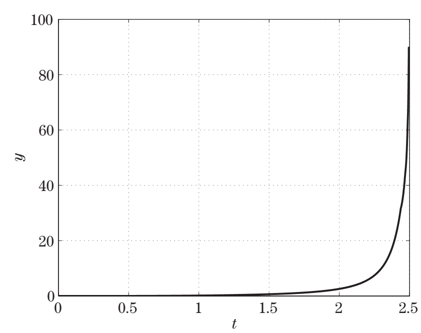

Figure 2 Case $c = 0$: results obtained by our methodology.

In Figure 3, we visualize for $c = 0.8$ and $t \in [0, 14.4]$ (the blow-up time being close to $T_{\max} \simeq 15.512$) the evolution of the computed approximations of the functions

$$u_{\ln} = \operatorname{sgn}(u)\ln(1 + |u|) \quad \text{and} \quad p_{\ln} = \operatorname{sgn}(p)\ln(1 + |p|) \tag{5.5}$$

restricted to the segment $\big\{\{x_1, x_2\},\ 0 \le x_1 \le 1,\ x_2 = \frac{1}{2}\big\}$. The oscillatory behavior of the solution appears clearly in Figure 3(b). In Figure 4, we report the graph of the computed approximations of u and p for $c = 0.8$ at $t = 15.512$, very close to the blow-up time.

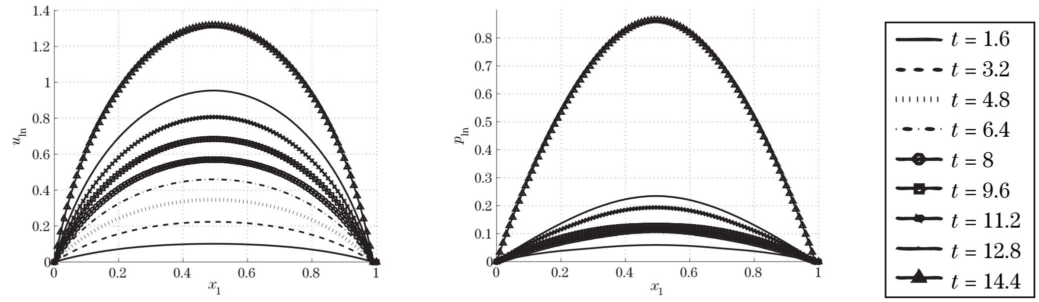

(a) evolution of $u_{\ln}$. (b) evolution of $p_{\ln}$. (c) caption.

Figure 3 Case $c = 0.8$, pure Dirichlet boundary conditions: Evolution of quantities (a) $u_{\ln}$ and (b) $p_{\ln}$. The caption in (c) is common to (a) and (b).

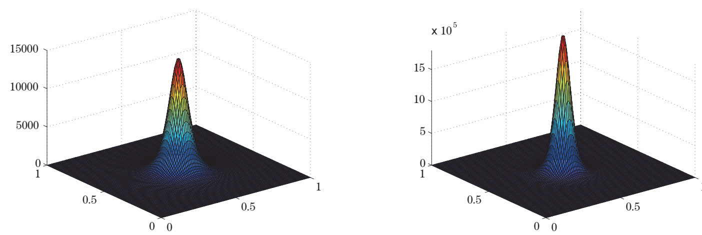

(a) u (b) p

Figure 4 Case $c = 0.8$, pure Dirichlet boundary conditions: Computed approximations for (a) u and (b) p at $t = 15.512$.

In Figure 5, we show for $c = 1$ the approximated evolution for $t \in [0, 35.03]$ of the function

$$t \to \max_{\{x,_1,x_2\}\in\Omega} u(x_1, x_2, t). \tag{5.6}$$

The computed maximum value is always achieved at $\{0.5, 0.5\}$. The explosive nature of the solution is obvious from this figure.

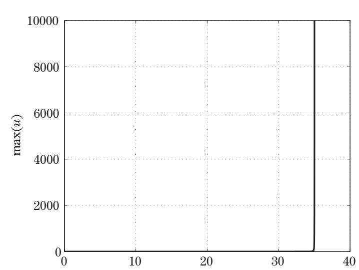

Figure 5 Case $c = 1$, pure Dirichlet boundary conditions: Evolution of the computed approximation of the function in (5.6) for $t \in [0, 35.03]$.

In order to better understand the evolution of the function (5.6), we analyze its restriction to the time interval $[0, 28]$ in both the time and frequency domains (see Figure 6). Actually, concerning the frequency domain, we specially analyze the modulation of the above function, that is the signal obtained after subtracting its convex component from the function in (5.6). Figure 6(b) indicates that the modulation observed in Figure 6(a) is quasi-monochromatic, with $f \simeq 0.9$ Hz.

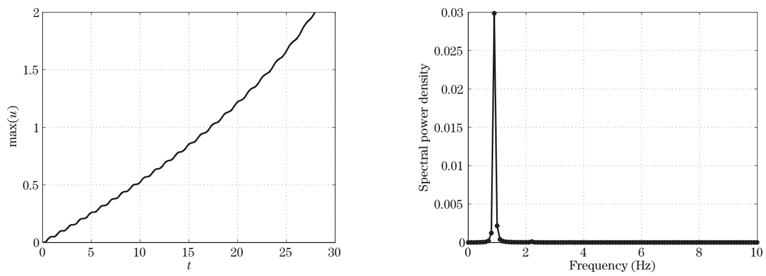

(a) Zoom of Figure 5. (b) Spectral power density for (a).

Figure 6 Case $c = 1$, pure Dirichlet boundary conditions: (a) evolution of the computed approximation of the function in (5.6) for $t \in [0, 28]$, (b) spectrum of the modulation.

Finally, Figure 7 reports the variation of the blow-up time of the approximated solution as a function of c. As mentioned above, the results obtained with $h = \frac{1}{100}$ and $h = \frac{1}{150}$ match very accurately.

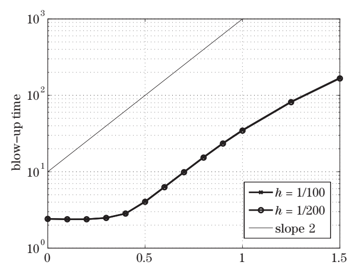

Figure 7 The blow-up time as a function of c (semi-log scale).

5.3 Numerical experiments for the nonlinear wave problem (1.2), (1.4)

The time discretization by operator-splitting of the nonlinear wave problem (1.2), (1.4) has been discussed in Subsection 2.3, where we showed that at each time step, we have to solve two nonlinear initial value problems such as (4.1) and one linear wave problem such as (3.1).

The simplicity of the geometry of this test problem (see Subsection 5.1) suggests the use of finite differences for the space discretization. Using the notation in Subsection 5.2, at each time step, we will have to solve $2I(I+1)$ initial value problem such as (4.1), that is two for each grid point M_{ij} $(1 \leq i \leq I+1,\, 1 \leq j \leq I)$. The solution method discussed in Section 4 is still valid. By discretizing problem (3.1) with finite differences, we obtain the following scheme:

$$\phi_{ij}^0 = \phi_0(M_{ij}), \quad 0 \leq i, j \leq I+1,$$
$$\phi_{ij}^1 - \phi_{ij}^{-1} = 2\tau\phi_1(M_{ij}), \quad 1 \leq i \leq I+1, 1 \leq j \leq I,$$

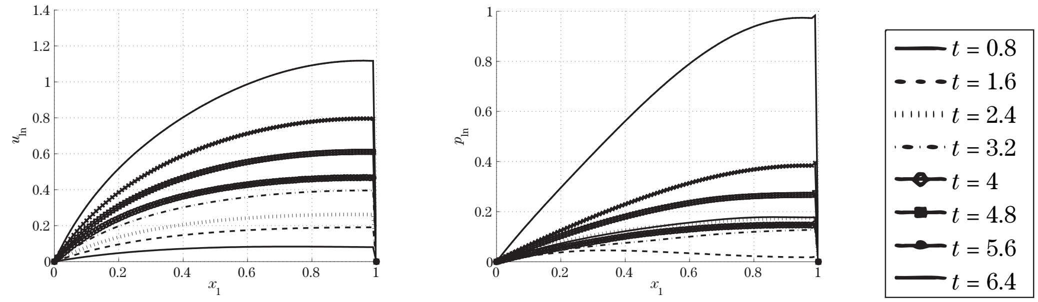

(a) evolution of $u_{\ln}$. (b) evolution of $p_{\ln}$. (c) caption.

Figure 8 Case $c = 0.8$, mixed Dirichlet-Sommerfeld boundary conditions: Evolution of quantities (a) $u_{\ln}$ and (b) $p_{\ln}$. The caption in (c) is common to (a) and (b).

then, for $q = 0, \cdots, Q$, $1 \le i \le I + 1, 1 \le j \le I$,

$$\begin{cases} \phi_{ij}^{q+1} + \phi_{ij}^{q-1} - 2\phi_{ij}^{q} + \beta\Big(\dfrac{\tau}{h}c\Big)^2(4\phi_{ij}^q - \phi_{i+1j}^q - \phi_{i-1j}^q - \phi_{ij+1}^q - \phi_{ij-1}^q) = 0, \\ \phi_{kl}^{q+1} = 0 \quad \text{if } M_{kl} \in \Gamma_0, \\ \dfrac{1}{\beta c}\dfrac{\phi_{I+1l}^{q+1} - \phi_{I+1l}^{q-1}}{2\tau} + \dfrac{\phi_{I+2l}^{q} - \phi_{Il}^{q}}{2h} = 0, \quad 1 \le l \le I, \end{cases} \tag{5.7}$$

where $\tau = \frac{t_f - t_0}{Q}$ and the "ghost" value ϕ_{I+2l}^q is introduced to impose the Sommerfeld condition at the discrete level. Upon elimination of ϕ_{I+2l}^q, we can derive a more practical formulation of the fully discrete problem, namely, for $q = 0, \cdots, Q$, $1 \le i \le I$, $1 \le j \le I$, instead of (5.7), we have

$$\begin{cases} \phi_{ij}^{q+1} + \phi_{ij}^{q-1} - 2\phi_{ij}^{q} + \beta\Big(\dfrac{\tau}{h}c\Big)^2(4\phi_{ij}^q - \phi_{i+1j}^q - \phi_{i-1j}^q - \phi_{ij+1}^q - \phi_{ij-1}^q) = 0, \\ \phi_{kl}^{q+1} = 0, \quad \text{if } M_{kl} \in \Gamma_0 \end{cases} \tag{5.8}$$

and for $q = 0, \cdots, Q$, $i = I + 1$, $1 \le j \le I$,

$$\begin{aligned} &\Big(1 + \frac{\tau}{h}c\Big)\phi_{I+1j}^{q+1} + \Big(1 - \frac{\tau}{h}c\Big)\phi_{I+1j}^{q-1} - 2\phi_{I+1j}^q \\ &+ \beta\Big(\frac{\tau}{h}c\Big)^2(4\phi_{I+1j}^q - 2\phi_{Ij}^q - \phi_{I+1j+1}^q - \phi_{I+1j-1}^q) = 0. \end{aligned} \tag{5.9}$$

Via (5.9), the discrete Sommerfeld boundary condition is included in the discrete wave equation.

We chose the same values for u_0, u_1, c, α, β, Q, h and Δt as in Subsection 5.2. Once again, the results obtained with $h = \frac{1}{100}$ and $h = \frac{1}{150}$ match very accurately.

In Figure 8, we visualize for $c = 0.8$ and $t \in [0, 6.4]$ (the blow-up time being close to $T_{\max} \simeq 7.432$) the evolution of the computed approximations of the quantities in (5.5) restricted to the segment $\big\{\{x_1, x_2\},\ 0 \le x_1 \le 1,\ x_2 = \frac{1}{2}\big\}$. These results (and the ones below) show that the blow-up occurs sooner than in the pure Dirichlet boundary condition case. In Figure 9, we report the graph of the computed approximations of u and p for $c = 0.8$ at $t = 7.432$, very close to the blow-up time.

Figure 10 reports the graph of the computed approximations of u and p for $c = 0.3$ at $t = 2.44$, very close to the blow-up time. Figures 9 and 10 show that for c sufficiently small (resp. large), the blow-up takes place inside Ω (resp. on Γ_1).

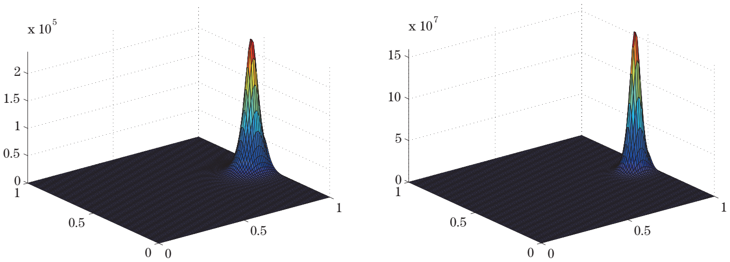

(a) u (b) p

Figure 9 Case $c = 0.8$, mixed Dirichlet-Sommerfeld boundary conditions: Computed approximations for (a) u and (b) p at $t = 7.432$.

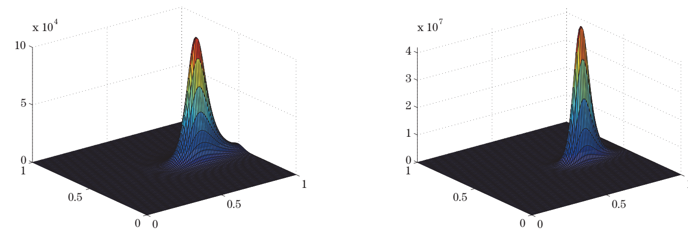

(a) u (b) p

Figure 10 Case $c = 0.3$, mixed Dirichlet-Sommerfeld boundary conditions: Computed approximations for (a) u and (b) p at $t = 2.44$.

In Figure 11(a), for $c = 1$, we report the approximated evolution of the function in (5.6) for $t \in [0, 15.135]$. In order to have a better view of the expected modulation of the above function, we report in Figure 11(b) its evolution for $t \in [0, 13.5]$. These figures show the dramatic growth of the solution as t gets closer to $T_{\max}$.

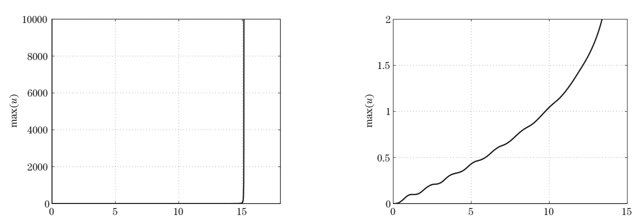

(a) function (5.6). (b) zoom of (a).

Figure 11 Case $c = 1$, mixed Dirichlet-Sommerfeld boundary conditions: (a) evolution of the computed approximation of the function in (5.6) for $t \in [0, 15.135]$, (b) zoomed view for $t \in [0, 13.5]$.

Finally, we report in Figure 12 the variation versus c of the blow-up time for both the pure Dirichlet and the mixed Dirichlet-Sommerfeld boundary conditions. It is interesting to observe how the presence of a boundary condition with (rather) good transparency properties decreases significantly the blow-up time, everything else being the same. Also, the above figure provides a strong evidence of the very good matching of the approximate solutions obtained for $h = \frac{1}{100}$

and $h = \frac{1}{150}$ (and the related time discretization steps).

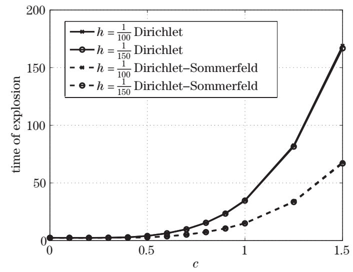

Figure 12 The blow-up time as a function of c for both the pure Dirichlet and the mixed Dirichlet-Sommerfeld boundary conditions.

6 Further Comments and Conclusions

The methods discussed in this article can be generalized to the coupling of the linear wave equation with other Painlevé equations, or other nonlinearities, such as $v \to e^v$. Actually, this claim is already validated by the results of numerical experiments, which we are performing with these other models. Another generalization under investigation is the application of the methods discussed here to the numerical solution to those nonlinear wave equations of the Euler-Poisson-Darboux type discussed in [19]. This application will require a 5-stage splitting scheme, instead of the 3-stage one, which we employed in this article.

We would like to conclude with the following two comments:

(1) When it goes to the numerical simulation of multi-physics phenomena, there are two possible approaches, namely, the monolithic (that is, un-split) methods and the operator-splitting methods. We think that the splitting methods discussed in this article are better suited for the solution to problems (1.2), (1.3) and (1.2), (1.4) than the monolithic ones.

(2) The splitting methods discussed in this article have good parallelization properties that we intend to investigate in the near future.

Acknowledgements The authors would like to thank the founders of the Painlevé Project. Their one page article in the Notices of the AMS [1] was the motivation of the work reported in this article. The authors thank Dr. Simone Paulotto for his help on the spectral analysis of some results.

References

[1] Bornemann, F., Clarkson, P., Deift, P., et al., A request: The Painlevé Project, *Notices of the American Mathematical Society*, **57**(11), 2010, 1938.

[2] Jimbo, M., Monodromy problem and the boundary condition for some Painlevé equations, *Publ. Res. Inst. Sci.*, **18**(3), 1982, 1137–1161.

[3] Wong, R. and Zhang, H. Y., On the connection formulas of the fourth Painlevé transcendent, *Analysis and Applications*, **7**(4), 2009, 419–448.

[4] Clarkson, P. A., Painlevé transcendents, NIST Handbook of Mathematical Functions, F. W. J. Olver, D. W. Lozier, R. F. Boisvert and C. W. Clark (eds)., Cambridge University Press, Cambridge, UK, 2010, 723–740.

[5] Fornberg, B. and Weideman, J. A. C., A numerical methodology for the Painlevé equations, *J. Comp. Phys.*, **230**(15), 2011, 5957–5973.

[6] Strang, G., On the construction and comparison of difference schemes, *SIAM J. Numer. Anal.*, **5**(3), 1968, 506–517.

[7] Glowinski, R., Finite element methods for incompressible viscous flow, Handbook of Numerical Analysis, Vol. IX, P. G. Ciarlet and J. L. Lions (eds.), North-Holland, Amsterdam, 2003, 3–1176.

[8] Bokil, V. A. and Glowinski, R., An operator-splitting scheme with a distributed Lagrange multiplier based fictitious domain method for wave propagation problems, *J. Comput. Phys.*, **205**(1), 2005, 242–268.

[9] Glowinski, R., Shiau, L. and Sheppard, M., Numerical methods for a class of nonlinear integro-differential equations, *Calcolo*, 2012, DOI: 10.1007/s10092-012-0056-2 (in press).

[10] Lions, J. L., Quelques Méthodes de Résolution des Problèmes aux Limites Non Linéaires, Dunod, Paris, 1969.

[11] Glowinski, R., Dean, E. J., Guidoboni, G., et al., Application of operator-splitting methods to the direct numerical simulation of particulate and free-surface flows and to the numerical solution to the two-dimensional elliptic Monge-Ampère equation, *Japan J. Indust. Appl. Math.*, **25**(1), 2008, 1–63.

[12] Chorin, A. J., Hughes, T. J. R., McCracken, M. F., et al., Product formulas and numerical algorithms, *Comm. Pure Appl. Math.*, **31**, 1978, 205–256.

[13] Beale, J. T. and Majda, A., Rates of convergence for viscous splitting of the Navier-Stokes equations, *Math. Comp.*, **37**(156), 1981, 243–259.

[14] Leveque, R. J. and Oliger, J., Numerical methods based on additive splittings for hyperbolic partial differential equations, *Math. Comp.*, **40**(162), 1983, 469–497.

[15] Marchuk, G. I., Splitting and alternating direction method, Handbook of Numerical Analysis, Vol. I, P. G. Ciarlet and J. L. Lions (eds.), North-Holland, Amsterdam, 1990, 197–462.

[16] Temam, R., Navier-Stokes Equations: Theory and Numerical Analysis, AMS Chelsea Publish, Providence, RI, 2001.

[17] Glowinski, R., Numerical Methods for Nonlinear Variational Problems, Springer-Verlag, New York, 1984.

[18] http://en.wikipedia.org/wiki/Painlevé_transcendents

[19] Keller, J. B., On solutions of nonlinear wave equations, *Comm. Pure Appl. Math.*, **10**(4), 1957, 523–530.